Molecular Therapy
Nucleic Acids
Original Article

lncRNA *SLC7A11-AS1* Promotes Chemoresistance by Blocking $SCF^{\beta\text{-}TRCP}$-Mediated Degradation of NRF2 in Pancreatic Cancer

Qingzhu Yang,[1] Kai Li,[1] Xuemei Huang,[1] Chen Zhao,[1] Yu Mei,[1] Xinyuan Li,[1] Lin Jiao,[1] and Huanjie Yang[1]

[1]School of Life Science and Technology, Harbin Institute of Technology, Harbin 150001, China

Drug resistance is the major obstacle of gemcitabine-based chemotherapy for the treatment of pancreatic ductal adenocarcinoma (PDAC). Many long non-coding RNAs (lncRNAs) are reported to play vital roles in cancer initiation and progression. Here, we report that lncRNA *SLC7A11-AS1* is involved in gemcitabine resistance of PDAC. *SLC7A11-AS1* is overexpressed in PDAC tissues and gemcitabine-resistant cell lines. Knockdown of *SLC7A11-AS1* weakens the PDAC stemness and potentiates the sensitivity of resistant PDAC cells toward gemcitabine *in vitro* and *in vivo*. *SLC7A11-AS1* promotes chemoresistance through reducing intracellular reactive oxygen species (ROS) by stabilizing nuclear factor erythroid-2-related factor 2 (NRF2), the key regulator in antioxidant defense. Mechanically, *SLC7A11-AS1* is co-localized with β-TRCP1 in the nucleus. The exon 3 of *SLC7A11-AS1* interacts with the F-box motif of β-TRCP1, the critical domain that recruits β-TRCP1 to the $SCF^{\beta\text{-}TRCP}$ E3 complex. This interaction prevents the consequent ubiquitination and proteasomal degradation of NRF2 in the nucleus. Our results demonstrate that the overexpression of *SLC7A11-AS1* in gemcitabine-resistant PDAC cells can scavenge ROS by blocking $SCF^{\beta\text{-}TRCP}$-mediated ubiquitination and degradation of NRF2, leading to a low level of intracellular ROS, which is required for the maintenance of cancer stemness. These findings suggest *SLC7A11-AS1* as a therapeutic target to overcome gemcitabine resistance for PDAC treatment.

INTRODUCTION

Pancreatic ductal adenocarcinoma (PDAC) is a highly aggressive malignancy, characterized by late diagnosis, low 5-year survival rate (9% for all stages), and resistance to chemotherapy.[1,2] Gemcitabine (2′, 2′-difluoro-2′-deoxycytidine [dFdC]) has been widely used for the treatment of locally advanced and metastatic PDAC; however, innate and acquired drug resistances have been major barriers in gemcitabine-based therapy.[3,4] Emerging evidence demonstrates that a subset of cancer cells, called cancer stem cells (CSCs), are highly resistant to chemotherapy and are responsible for drug resistance and cancer recurrence. Gemcitabine eliminates the bulk cancer cells, leading to enrichment of the CSCs in PDAC.[5] A low level of intracellular reactive oxygen species (ROS) is required for the maintenance of cancer stemness.[6] Chemotherapeutic agents such as gemcitabine stimulate ROS generation to induce cell death.[4] To survive under oxidative stress, chemoresistant cancer cells develop an effective antioxidant system to limit the excessive accumulation of ROS.[7] Nuclear factor erythroid-2-related factor 2 (NRF2), the key regulator of redox hemostasis, is frequently observed to be overexpressed in CSCs in contrast with the bulk cancer cells.[8] In addition, NRF2 is overexpressed in PDAC tissues and confers their chemoresistance.[9,10] NRF2 is tightly regulated by the ubiquitin-proteasome system.[11] Two major E3 ligases are involved in NRF2 proteasomal degradation: the KEAP1-Cul3-Rbx1 and the SKP1-Cul1-Rbx1 ($SCF^{\beta\text{-}TRCP}$) E3 complex, which mediate NRF2 ubiquitination and subsequent degradation in the cytosol and nucleus, respectively.[12,13] Intriguingly, NRF2 protein level is not negatively correlated to the KEAP1 expression in PDAC.[9] In addition, the sustained activation of NRF2 in human PDAC cannot be explained by somatic mutations in NRF2 or KEAP1.[14] Furthermore, high levels of β-TRCP1 are also detected in the specimens of PDAC.[15] Thus, it is necessary to find the underlying mechanism responsible for elevated levels of NRF2 in PDAC, which might be of potential therapeutic value in overcoming gemcitabine resistance.

Long non-coding RNAs (lncRNAs) provide a new perspective in understanding complicated signal transduction. They are transcribed by polymerase II with greater than 200 nt. Increasing evidence demonstrates the crucial roles of lncRNAs in the tumorigenesis and chemoresistance of PDAC.[16–20] For example, *Neat1* has been reported to suppress pancreatic cancer initiation in a p53-dependent manner.[18] lncRNA *MALAT-1* (metastasis-associated lung adenocarcinoma transcript 1) was found to promote tumorigenicity and reduce chemosensitivity of PDAC cells.[19] Our previous work indicates that linc-*DYNC2H1-4* promotes PDAC stemness by acting as a sponge of miR-145.[20]

Received 4 November 2019; accepted 5 November 2019;
https://doi.org/10.1016/j.omtn.2019.11.035.

Correspondence: Huanjie Yang, School of Life Science and Technology, Harbin Institute of Technology, Harbin, China.
E-mail: yanghj@hit.edu.cn

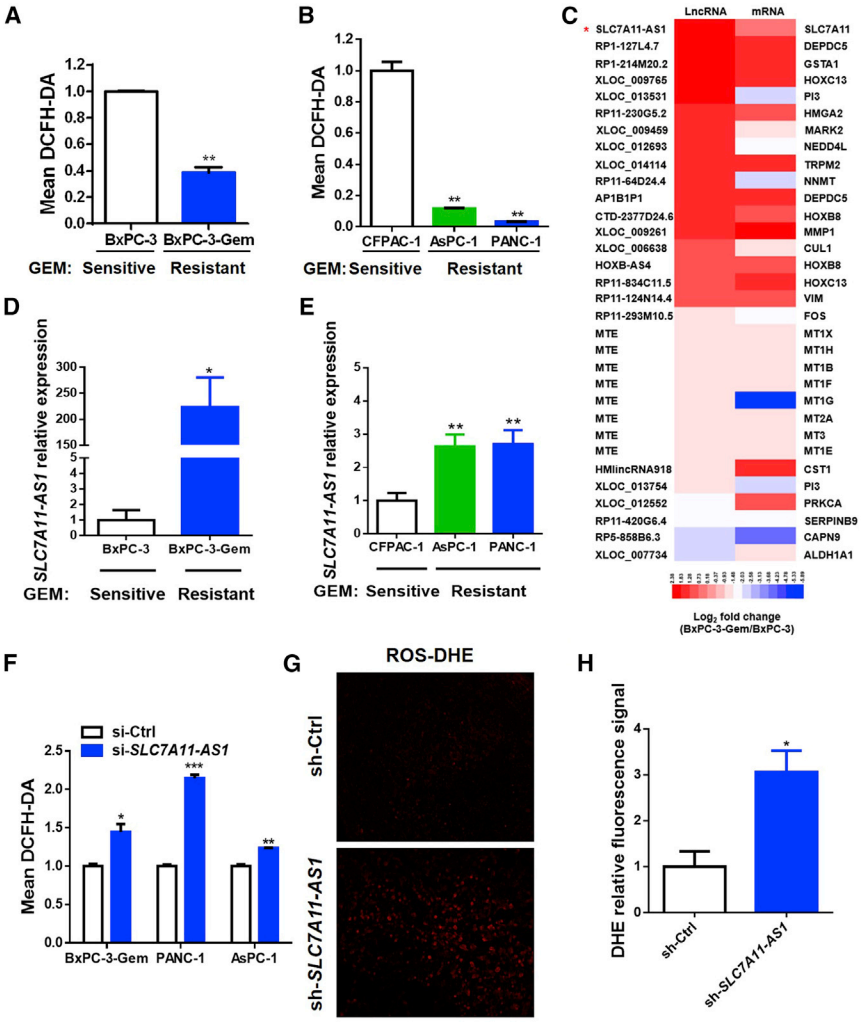

Figure 1. Overexpression of *SLC7A11-AS1* in Gemcitabine-Resistant PDAC Cells Reduces Intracellular ROS Level

(A and B) PDAC cells with acquired (A, BxPC-3-Gem *vs* BxPC-3) or innate (B, PANC-1 and AsPC-1 *vs* CFPAC-1) gemcitabine resistance were incubated with probe DCFH-DA (10 μM) for 30 min. ROS levels were detected by flow cytometry. (C) The log2 fold changes of lncRNAs and their nearby coding genes that are associated with ROS regulation were presented by heatmap. (D and E) Expression of *SLC7A11-AS1* in PDAC cell lines with aquired (D) or innate drug resistance (E) was detected by qRT-PCR and normalized to GAPDH (n = 3). (F) ROS levels were determined in gemcitabine-resistant PDAC cells with *SLC7A11-AS1* knockdown or control as described in (A) and (B). (G and H) *SLC7A11-AS1*-knockdown and control PANC-1 cells (1.5×10^6) were inoculated in BALB/c nude mice (n = 5). Slides from tumor tissues were incubated with DHE for *in situ* detection of ROS. (G and H) Fluorescence was detected by fluorescent microscope (G) and quantified by using ImageJ (H) (n = 3). *p < 0.05, **p < 0.01, ***p < 0.001.

In this study, we found that lncRNA *SLC7A11-AS1* was overexpressed in gemcitabine-resistant PDAC cells and was involved in drug resistance. It interacts with the F-box motif of β-TRCP1, preventing NRF2 ubiquitination and subsequent proteasomal degradation in the nucleus, which in turn reduces intracellular ROS for the maintenance of PDAC stemness and chemoresistance.

RESULTS

Overexpression of *SLC7A11-AS1* in Gemcitabine-Resistant PDAC Cells Reduces the Intracellular Level of ROS

Previously, we established a gemcitabine-resistant subline BxPC-3-Gem (Figure S1A) from the parental sensitive pancreatic cancer BxPC-3 cells and found that gemcitabine-resistant PDAC cells had high cancer stemness properties.[20] Because a low level of ROS is required for the maintenance of stemness,[6] we determined the ROS level in this paired cell line and found that it was lower in gemcitabine-resistant BxPC-3-Gem than that in the sensitive cells (Figure 1A). Low levels of intracellular ROS were also observed in the other two gemcitabine-resistant cell lines, PANC-1 and AsPC-1 (Figure S1B), in comparison with the sensitive CFPAC-1 cells (Figure 1B). To see lncRNA involvement in ROS regulation, we performed array analysis and enriched lncRNAs with potential involvement in ROS regulation according to the nearby associated genes. Among them, lncRNA *SLC7A11-AS1* was the gene that was in highest expression in BxPC-3-Gem compared with BxPC-3 cells (Figure 1C). qRT-PCR confirmed that *SLC7A11-AS1* was overexpressed in BxPC-3-Gem compared with BxPC-3 cells (Figure 1D). Different expression levels of *SLC7A11-AS1* were also observed in gemcitabine-resistant PANC-1 and AsPC-1 in comparison with the sensitive CFPAC-1 cells (Figure 1E). Next, we knocked down *SLC7A11-AS1* in gemcitabine-resistant cell lines to determine its effect in ROS regulation. Three small interfering RNAs (siRNAs) were designed, and siRNA#1 could knock down *SLC7A11-AS1* expression by 50% (Figure S1C); thus, it was used in further study. Knockdown of *SLC7A11-AS1* in gemcitabine-resistant BxPC-3-Gem, PANC-1, and AsPC-1 cells (Figure S1D) led to significant elevation of intracellular ROS levels (Figure 1F), indicating that *SLC7A11-AS1* acts as an antioxidant. To see the *in vivo* effect, PANC-1 cells with *SLC7A11-AS1*-knockdown or control shRNA (Figure S1E) were subcutaneously inoculated into BALB/c nude mice. PANC-1 xenograft tissues with *SLC7A11-AS1* knockdown showed near 3-fold increase of ROS levels in comparison with control (Figures 1G and 1H). These results indicate that overexpression of *SLC7A11-AS1* in gemcitabine-resistant PDAC cells can reduce the intracellular level of ROS.

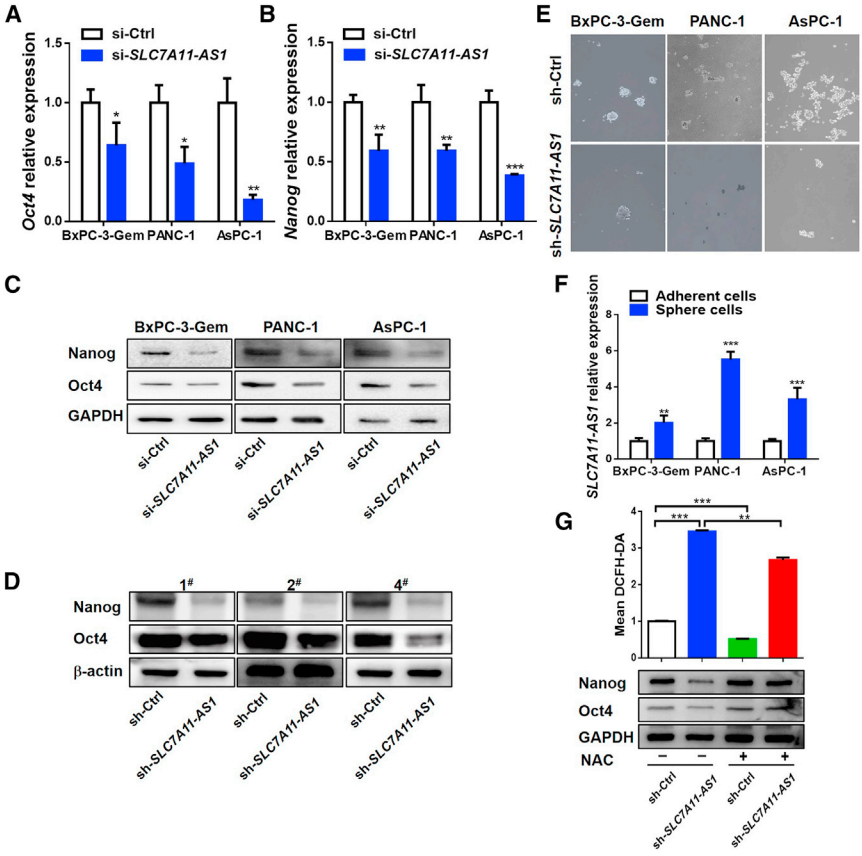

Figure 2. *SLC7A11-AS1* Scavenges ROS to Promote Cancer Stemness

(A–C) Effects of *SLC7A11-AS1* knockdown on expressions of Oct4 and Nanog were determined by qRT-PCR (A and B) and western blot (C) in gemcitabine-resistant PDAC cells (n = 3). (D) Expressions of Oct4 and Nanog in tumor tissues (as described in Figure 1G) were determined by western blot (D). (E) Oncosphere-formation assay in *SLC7A11-AS1*-knockdown and control gemcitabine-resistant PDAC cells. Original magnification ×10. (F) qRT-PCR analysis of *SLC7A11-AS1* expression in spheroids and paired attached PDAC cells (n = 3). (G) Flow cytometry analysis of ROS using probe DCFH-DA (upper) and western blot analysis of Oct4 and Nanog (bottom) in *SLC7A11-AS1*-knockdown and control PANC-1 cells treated with or without NAC (10 mM) for 48 h (n = 3). *p < 0.05, **p < 0.01, ***p < 0.001.

SLC7A11-AS1 Scavenges ROS to Promote Cancer Stemness

Because a low level of ROS is required for the maintenance of cancer stemness,[6] we further investigated whether *SLC7A11-AS1* could affect cancer stemness. *Oct4* and *Nanog*, the two markers of stemness, were significantly decreased in *SLC7A11-AS1*-knockdown BxPC-3-Gem, PANC-1, and AsPC-1 cells (Figure S1D) in comparison with control at both mRNA and protein levels (Figures 2A–2C). *In vivo*, the tumors derived from the *SLC7A11-AS1* knockdown group exhibited lower protein levels of Nanog and Oct4 than the control group (Figure 2D). Knockdown of *SLC7A11-AS1* in the three gemcitabine-resistant cell lines by shRNA (Figure S1E) significantly suppressed their sphere-forming abilities, a representative trait of CSCs[21] (Figure 2E). In addition, compared with the adherent cells, the spheroids exhibited higher expression level of *SLC7A11-AS1* (Figure 2F). These results indicate that *SLC7A11-AS1* promotes cancer stemness in PDAC cells.

Then we further determined whether *SLC7A11-AS1* promotes cancer stemness through reducing ROS level. We introduced *N*-acetylcysteine (NAC), a scavenger of ROS. The use of NAC decreased *SLC7A11-AS1* silencing-induced ROS (Figure 2G, upper), which also reduced its impact on stemness. *SLC7A11-AS1* silencing-induced protein decreases of Nanog and Oct4 were rescued to control level by addition of NAC (Figure 2G, bottom), indicating that *SLC7A11-AS1* regulates cancer stemness via regulating ROS level in gemcitabine-resistant PDAC cells.

SLC7A11-AS1 Promotes Chemoresistance in PDAC

Cancer stemness confers chemoresistance.[22] Next, we investigated *SLC7A11-AS1* involvement in chemoresistance. Knockdown of *SLC7A11-AS1* caused growth inhibition and further potentiated gemcitabine efficacy in resistant BxPC-3-Gem, PANC-1, and AsPC-1 cells (Figures 3A–3C). Moreover, colony formation showed an almost 2-fold decrease of colony numbers after gemcitabine treatment in *SLC7A11-AS1*-knockdown BxPC-3-Gem, PANC-1, and AsPC-1 cells compared with control (Figures 3D and 3E). To see *SLC7A11-AS1* effects *in vivo*, PANC-1 xenografts with *SLC7A11-AS1* knockdown or control were established subcutaneously in BALB/c mice, followed by gemcitabine treatment every 4 days when control tumor reached 150 mm^3. *SLC7A11-AS1* knockdown significantly potentiated gemcitabine efficacy as shown by the approximately 80% decrease of tumor growth and 77% decrease of tumor weight in the *SLC7A11-AS1*-knockdown plus gemcitabine group in comparison with gemcitabine alone group (Figures 3F and 3G). These results indicate that *SLC7A11-AS1* can potentiate cancer cell sensitivity toward gemcitabine, suggesting it might be of potential therapeutic value to overcome gemcitabine resistance in PDAC.

SLC7A11-AS1 Correlates with Poor Prognosis of PDAC Patients

To see the clinical significance of *SLC7A11-AS1*, we determined *SLC7A11-AS1* expressions in PDAC patients and found that it was higher in tumor tissues than that in the adjacent normal tissues (n = 27) (Figure 4A). A large-scale dataset analysis by using Gene Expression Profiling Integrative Analysis (GEPIA; http://gepia.cancer-pku.cn)[23] confirmed that *SLC7A11-AS1* was overexpressed in PDAC tissues (n = 179) compared with normal tissues (n = 171) (p < 0.01) (Figure 4B). Moreover, Kaplan-Meier survival analysis indicated that high expression of *SLC7A11-AS1* in PDAC tissues was associated with a shorter overall lifespan of PDAC patients

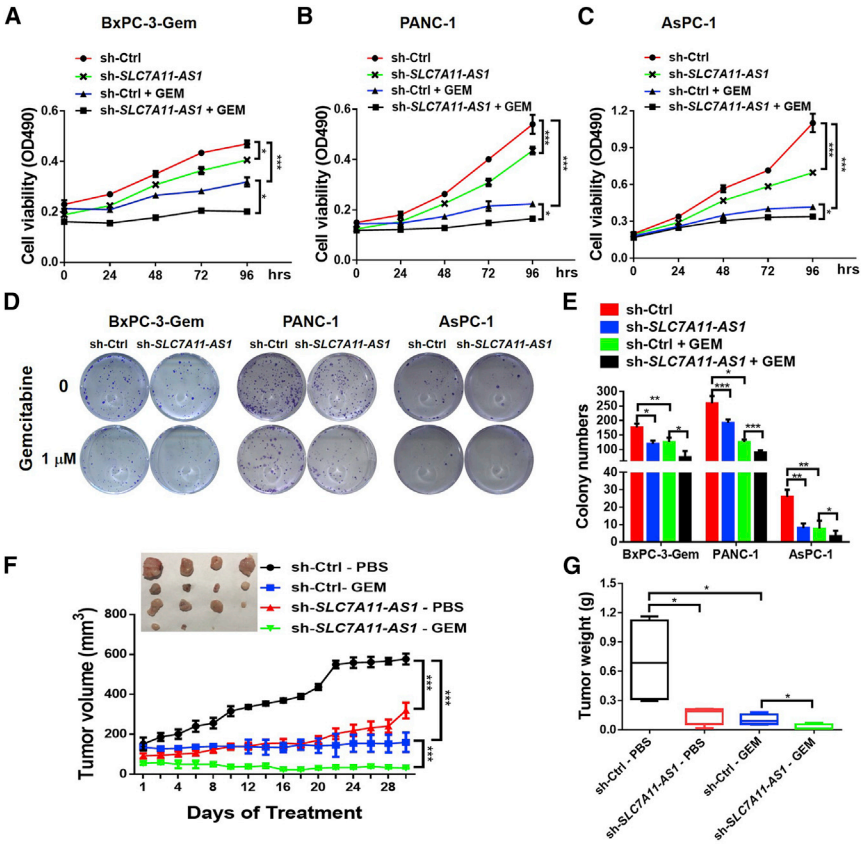

Figure 3. *SLC7A11-AS1* Knockdown Potentiates Resistant PDAC Cell Response to Gemcitabine

(A–C) *SLC7A11-AS1*-knockdown and control (A) BxPC-3-Gem, (B) PANC-1, and (C) AsPC-1 cells were treated with gemcitabine (1 μM) for indicated times, and cell viability was analyzed by MTT assay (n = 3). (D and E) Colony formation assays of *SLC7A11-AS1*-knockdown and control cells with gemcitabine treatment (1 μM) for 2 weeks (n = 3). Representative images (D) and average number of colonies (E) were shown. (F and G) Subcutaneous xenograft analysis of *SLC7A11-AS1*-knockdown and control PANC-1 cells (1.5×10^6) in nude mice treated with gemcitabine (50 mg/kg body weight) or PBS by intraperitoneal (i.p.) injection every 4 days (n = 4). Tumor volume (F) and weight (G) were shown. *p < 0.05, **p < 0.01, ***p < 0.001.

(p = 0.027) (Figure 4C), indicating that high level of *SLC7A11-AS1* correlates with poor prognosis of PDAC patients.

SLC7A11-AS1 Prevents NRF2 Proteasomal Degradation to Defend ROS

Next, we were interested to know how *SLC7A11-AS1* affected ROS level in PDAC cells. NRF2 is the key regulator of redox homeostasis.[24] We noticed that NRF2 protein level was in line with the endogenous expression level of *SLC7A11-AS1*, showing that PDAC cells (BxPC-3-Gem, PANC-1, and AsPC-1) with highly expressed *SLC7A11-AS1* had high protein levels of NRF2, and conversely, cells with lowly expressed *SLC7A11-AS1* had low protein levels of NRF2 (Figure 5A versus Figures 1D and 1E). These results suggest that *SLC7A11-AS1* might regulate NRF2 in PDAC cells. Knockdown of *SLC7A11-AS1* in *SLC7A11-AS1*-overexpressed BxPC-3-Gem, PANC-1, and AsPC-1 cells had no effect on *NRF2* mRNA levels (Figure 5B). However, it led to reduction of NRF2 protein in the three gemcitabine-resistant PDAC cells (Figure 5C). Then we determined whether *SLC7A11-AS1* might affect the stability of NRF2 protein. We treated the cells with protein synthesis inhibitor cycloheximide (CHX) and found that knockdown of *SLC7A11-AS1* reduced the stability of NRF2 protein (Figures 5D and 5E). The half-life of NRF2 protein was shortened by about 3-fold by *SLC7A11-AS1* knockdown in PANC-1 cells (Figure 5E). Subcellular fractionation revealed that the nuclear portion of NRF2 protein was significantly decreased upon *SLC7A11-AS1* knockdown, but not the cytosolic portion (Figures 5F and 5G). MG132, a specific proteasome inhibitor, could completely rescue the loss of nuclear NRF2 protein caused by *SLC7A11-AS1* knockdown (Figures 5H and 5I), indicating that *SLC7A11-AS1* stabilizes nuclear NRF2 by preventing its proteasomal degradation.

Then, we determined whether *SLC7A11-AS1* exhibited antioxidant ability through NRF2 regulation. Flow cytometry (FCM) analysis showed that ectopic expression of *SLC7A11-AS1* caused ROS reduction, whereas it lost antioxidant function when NRF2 was silenced by siRNA (Figure 5J). NRF2 activates the expressions of target antioxidant genes such as *GCLM* and *HMOX1*.[25,26] qRT-PCR showed that ectopic expression of *SLC7A11-AS1* upregulated the expressions of *GCLM* and *HMOX1*, whereas the upregulations were decreased to or even under basal level when *NRF2* was knocked down (Figures 5K and 5L). These results indicate that *SLC7A11-AS1* prevents the proteasomal degradation of nuclear NRF2, leading to decreased ROS.

SLC7A11-AS1 Interacts with β-TRCP1 to Block NRF2 Ubiquitination in the Nucleus

To see the underlying mechanism that *SLC7A11-AS1* prevents NRF2 proteasomal degradation in the nucleus, we determined the intracellular location of *SLC7A11-AS1* in BxPC-3-Gem and PANC-1 cells. qRT-PCR showed that *SLC7A11-AS1* was mainly located in the nucleus, and it was marginally detected in the cytosol (Figures 6A and 6B). Considering that *SLC7A11-AS1* regulates NRF2 posttranscription and lncRNAs within the nucleus function through protein interaction,[27,28] we hypothesized that *SLC7A11-AS1* might be interfering with a nuclear E3 ligase to affect the stability of NRF2. β-TRCP1 is reported to be responsible for NRF2 ubiquitination and proteasomal degradation in the nucleus.[13] Therefore, we performed nuclear co-localization of β-TRCP1 with *SLC7A11-AS1*. Immunofluorescence

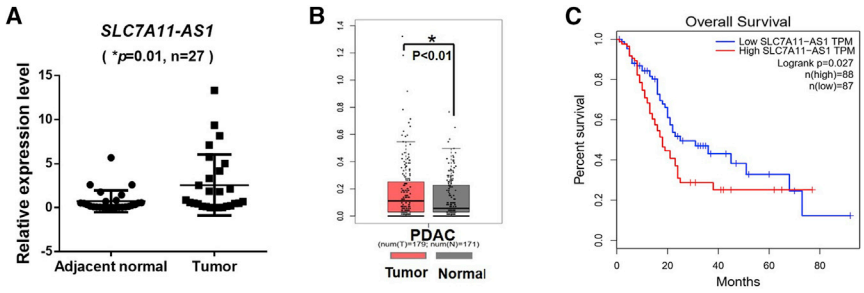

Figure 4. *SLC7A11-AS1* Expression Levels Are Correlated with PDAC Patient's Survival

(A) Expression of *SLC7A11-AS1* in tumor and adjacent normal tissues of PDAC patients was determined by qRT-PCR and normalized to 18S rRNA (n = 27). (B) The expression level of *SLC7A11-AS1* in PDAC and normal tissues was analyzed by using GEPIA. (C) Kaplan-Meier curve of overall survival of PDAC patients analyzed by using GEPIA.

showed that β-TRCP1 and *SLC7A11-AS1* were co-localized in the nucleus of BxPC-3-Gem and PANC-1 cells (Figure 6C).

To see whether *SLC7A11-AS1* could interact with β-TRCP1, nuclear extracts from BxPC-3-Gem cells were incubated with biotinylated sense or antisense *SLC7A11-AS1* RNA generated *in vitro*. Proteins precipitated with streptavidin beads were resolved by SDS-PAGE. The association of β-TRCP1 with *SLC7A11-AS1* sense RNA, but not antisense or the beads, was confirmed by immunoblotting analysis with anti-β-TRCP1 antibody (Figure 6D). To identify the regions of *SLC7A11-AS1* that are responsible for binding with β-TRCP1, we generated five fragments of *SLC7A11-AS1* (Figure 6E). The results from RNA pull-down and immunoblotting showed that *SLC7A11-AS1* exon 3 (440–1,725 nt of *SLC7A11-AS1*) was essential for the interaction with β-TRCP1 protein (Figure 6F). Reciprocally, RNA immunoprecipitation (RIP) assay was performed to confirm the interaction between *SLC7A11-AS1* and β-TRCP1. β-TRCP1 has two major domains: the F-box domain, which is responsible for recruiting β-TRCP1 to the SKP1-Cul1-Rbx1 ($SCF^{β\text{-}TRCP}$) E3 ligase complex through interaction with adaptor protein SKP1; and the WD domain responsible for interaction with the substrates.[29] To see which domain is responsible for interacting with *SLC7A11-AS1*, β-TRCP1 fragments with deletions of either one (β-TRCP1-N without WD domain and β-TRCP1-C without F-box motif) or both domains (β-TRCP1-N-ΔF-box) were constructed (Figure 6G). Western blot using input lysates from PANC-1 cells transfected with hemagglutinin (HA)-tagged β-TRCP1 and its truncations confirmed their expressions (Figure 6H, left). The immunoprecipitates revealed that *SLC7A11-AS1* was enriched by β-TRCP1 antibody. Almost 50% of input *SLC7A11-AS1* could be pulled down by full-length β-TRCP1 (Figure 6H, right). However, β-TRCP1 fragment without F-box domain (β-TRCP1-C, containing WD) completely lost its interaction with *SLC7A11-AS1*, showing a *SLC7A11-AS1* level similar to empty vector. β-TRCP1 fragment without WD domain (β-TRCP1-N, containing F-box motif) could interact with *SLC7A11-AS1*, but its binding ability dropped nearly 40% compared with the full-length β-TRCP1 (Figure 6H, right). Further deletion showed that β-TRCP1 fragment without both F-box and WD domains (β-TRCP1-N-ΔF-box) was not able to interact with *SLC7A11-AS1*; the binding activity dropped ~90% (Figure 6H, right). These results demonstrate that the F-box domain of β-TRCP1 is responsible for its direct interaction with *SLC7A11-AS1*, but it needs the WD domain to enhance the binding ability.

Next, we determined whether the interaction between *SLC7A11-AS1* and β-TRCP1 was functional. As shown in Figure 6I, β-TRCP1 led to NRF2 ubiquitination, but it was blocked in the presence of *SLC7A11-AS1* in 293T cells (Figure 6I), indicating that the interaction between *SLC7A11-AS1* and β-TRCP1 blocks NRF2 ubiquitination. The F-box domain is responsible for β-TRCP1 interacting with SKP1 of the $SCF^{β\text{-}TRCP1}$ E3 complex. If this domain was blocked by *SLC7A11-AS1*, the degradation of other substrates of $SCF^{β\text{-}TRCP1}$ E3 would be affected as well. Indeed, we found that the proteasomal degradation of nuclear β-catenin, another substrate of $SCF^{β\text{-}TRCP1}$,[30] was blocked by *SLC7A11-AS1* (Figure 6J), further confirming that *SLC7A11-AS1* interacts with the F-box of β-TRCP1.

DISCUSSION

lncRNAs play important roles in governing cell response to chemotherapeutics.[31,32] In the current study, we found that *SLC7A11-AS1* promotes cancer stemness and chemoresistance by scavenging ROS. *SLC7A11-AS1* stabilizes nuclear NRF2 protein by blocking $SCF^{β\text{-}TRCP}$-mediated ubiquitination and subsequent proteasomal degradation, leading to a low level of intracellular ROS, which is required for the maintenance of PDAC stemness and chemoresistance (Figure 7).

SLC7A11-AS1 is the anti-sense transcript of *SLC7A11* that encodes xCT, a transporter of glutamine and cysteine.[33] It has been reported as a tumor suppressor in gastric and epithelial ovarian cancer, which is downregulated in these tumor tissues compared with the adjacent non-tumorous counterparts.[33,34] Our data indicate that *SLC7A11-AS1* is an oncogene in PDAC that contributes to spheroformation and the upregulation of CSC markers. Furthermore, overexpression of *SLC7A11-AS1* confers to gemcitabine resistance of PDAC cells both *in vitro* and *in vivo*. High expressions of *SLC7A11-AS1* are detected in human PDAC specimens and associate with a shorter overall lifespan of PDAC patients, further supporting the oncogenic function of *SLC7A11-AS1* in PDAC. The discrepancy of *SLC7A11-AS1* function in gastric, epithelial ovary cancer and PDAC might be because of different cancer types.

Accumulating evidence has demonstrated that CSCs are responsible for tumorigenesis, chemoresistance, metastasis, and progression,[35] and a low level of ROS is required for the maintenance of cancer stemness.[6] PDAC cells resistant to gemcitabine exert enhanced property of cancer stemness.[20,36] Here, we found that the resistant

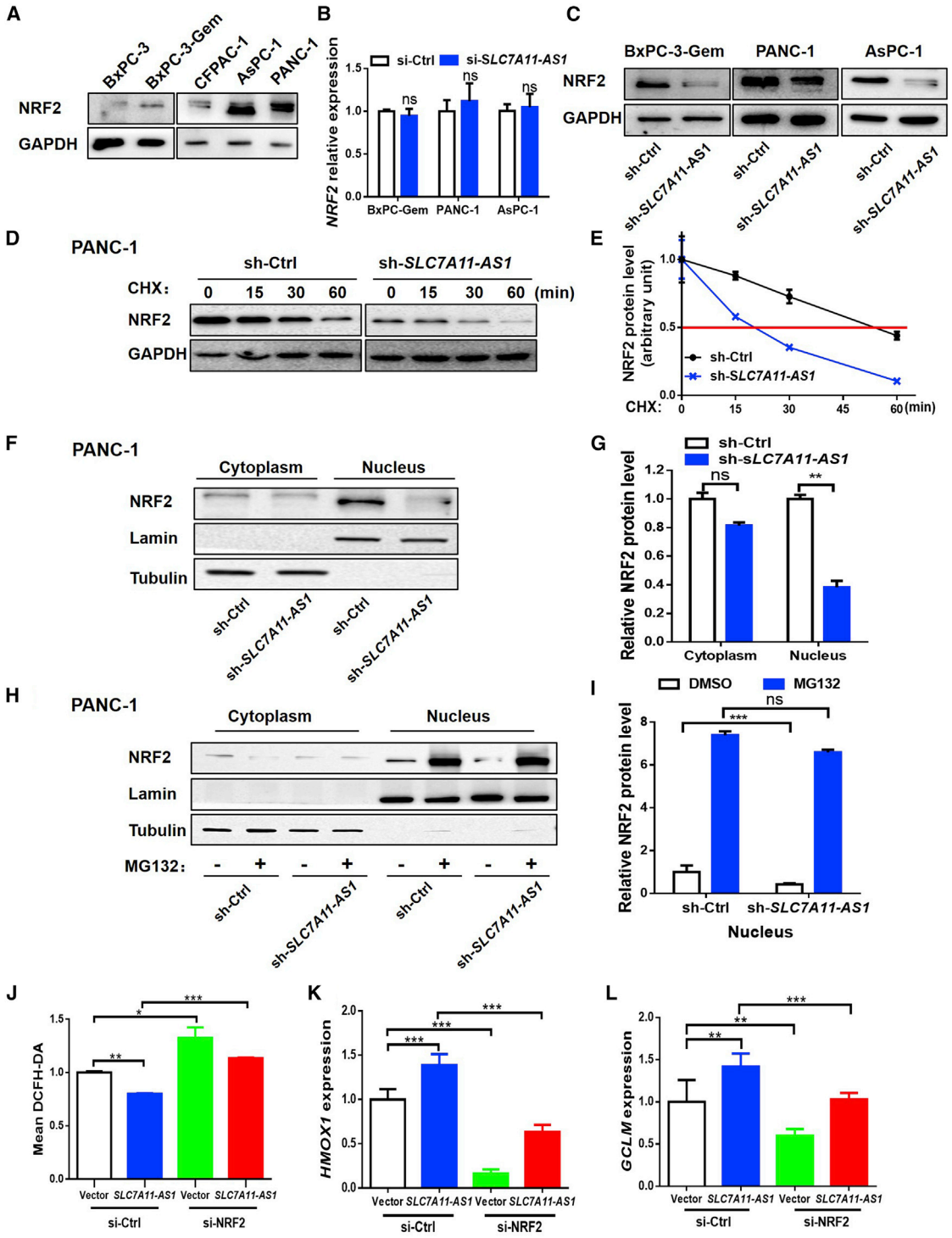

Figure 5. *SLC7A11-AS1* Prevents NRF2 Proteasomal Degradation to Defend ROS

(A) Western blot analysis of NRF2 in PDAC cell lines. (B and C) Effects of *SLC7A11-AS1* knockdown on NRF2 expression were determined by qRT-PCR (B) and western blot (C) in *SLC7A11-AS1*-overexpressed PDAC cells (n = 3). (D) Effect of *SLC7A11-AS1* knockdown on half-life of NRF2 was determined by western blot in PANC-1 cells treated with CHX (100 μg/mL). (E) Quantification of NRF2 was normalized to the loading control and expressed relative to 0 h. (F) NRF2 protein levels in the nucleus and cytosol in PANC-1 cells with *SLC7A11-AS1* knockdown or sh-Ctrl were determined by western blot. (G) Quantifications of nuclear and cytoplasmic NRF2 were normalized to the

(legend continued on next page)

PDAC cells also showed a decreased level of ROS in comparison with the sensitive cells. *SLC7A11-AS1* is overexpressed in gemcitabine-resistant PDAC cells. Knockdown of *SLC7A11-AS1* results in elevation of the intracellular ROS, leading to the loss of stemness. *SLC7A11-AS1* silencing-induced reduction of stemness can be rescued by NAC, a scavenger of ROS. These results indicate that *SLC7A11-AS1* plays a role in the maintenance of cancer stemness by suppressing ROS. Furthermore, our results demonstrate that *SLC7A11-AS1* exerts antioxidant activity through NRF2. It lost antioxidant function when NRF2 was silenced.

NRF2 is the key regulator of antioxidant defense.[8] Overactivation of NRF2 promotes cancer cell survival and enhances cancer stemness, as well as chemoresistance and/or radioresistance.[37] Dysregulation on the ubiquitin-proteasomal degradation of NRF plays an important role in the sustained activation of NRF2 in cancers. For example, KEAP1 methylation leads to reduced KEAP1 level, which correlates with increased level of nuclear NRF2 in colon cancer.[38] Somatic mutation of NRF2 or KEAP1 that disrupts NRF2/KEAP1 interaction confers to NRF2 activation in renal cell carcinoma and other types of solid tumors.[39,40] Recently, β-TRCP has been identified as an E3 ligase that mediates NRF2 degradation in the nucleus.[41] β-TRCP belongs to the F-box protein families, also known as F-box/WD repeat-containing protein 1A (FBXW1A).[29] It consists of two major functional domains: the carboxy-terminal WD domain that binds to specific substrates; and the F-box motif, which recruits F-box protein to the SKP1-Cul1-Rbx1 ($SCF^{\beta\text{-}TRCP}$) E3 ligase complex through interaction with adaptor protein SKP1.[29] β-TRCP recognizes and binds to the DSGIS and DSAPGS motifs in the Neh6 domain of NRF2 and ubiquitylates NRF2 for proteasome degradation in the nucleus.[13,41] NRF2 protein in normal pancreatic ductal epithelial cells is defined in the cytosol at weak level and without nuclear expression. It shows increased cytoplasmic level and positive staining in the nucleus in PDAC tissues.[9] However, NRF2 protein level is not negatively correlated to the KEAP1 expression in PDAC tissues.[9] In addition, the sustained activation of NRF2 in human PDAC cannot be explained by somatic mutations of NRF2 or KEAP1.[14] Furthermore, high levels of β-TRCP1 are also detected in the specimens of PDAC.[15] Hence it is necessary to find an additional degradation mechanism to understand sustained activation of NRF2 in PDAC. In the present study, our results reveal that the overexpression of *SLC7A11-AS1* in gemcitabine-resistant PDAC cells can block β-TRCP1-mediated ubiquitination and subsequent degradation of NRF2. *SLC7A11-AS1* is co-localized with β-TRCP1 in the nucleus of PDAC cells. Pull-down assays show that β-TRCP1 binds to exon 3 (440–1725 nt) of *SLC7A11-AS1*. RIP assays reveal that *SLC7A11-AS1* interacts with the F-box domain of β-TRCP1. Moreover, *SLC7A11-AS1* blocks β-TRCP1-mediated ubiquitination and subsequent proteasomal degradation of NRF2 in the nucleus of PDAC cells. There is another mechanism reported to affect the stability of nuclear NRF2. NRF2 traffics to promyelocytic leukemia-nuclear bodies (PMLNBs), where RNF4 polyubiquitylates polysumoylated NRF2 in PML-NBs, subsequently leading to its degradation.[42] In this study, we cannot rule out whether *SLC7A11-AS1* might affect RNF4-mediated nuclear NRF2 degradation. However, our results clearly demonstrate that *SLC7A11-AS1* is involved in $SCF^{\beta\text{-}TRCP}$-mediated NRF2 degradation in the nucleus.

β-TRCP plays critical roles in many key processes, such as cell cycle, apoptosis, and migration.[43] A number of important proteins, including β-catenin, cell division cycle 25 (Cdc25), vascular endothelial growth factor receptor 2 (VEGFR2), inhibitor of nuclear factor-κB (IκB), and mouse double minute 2 (Mdm2), are ubiquitinated by β-TRCPs.[29] Given that *SLC7A11-AS1* binds to the F-box domain of β-TRCP1, which is responsible for recruiting β-TRCP1 to the $SCF^{\beta\text{-}TRCP}$ E3 complex, it raises a possibility that *SLC7A11-AS1* may inhibit ubiquitination and degradation of other substrates of β-TRCP1. Indeed, we found that knockdown of *SLC7A11-AS1* led to enhanced degradation of nuclear β-catenin, further supporting that *SLC7A11-AS1* interacts with the F-box domain of β-TRCP1, blocking the formation of the SKP1-Cul1-Rbx1 E3 ligase complex. Hence *SLC7A11-AS1* is a very important lncRNA that can affect the degradation of extensive substrates of β-TRCP1. Several lncRNAs have been reported to interfere with E3 ligase, such as *OCC-1*[44] and *UPAT*.[45] These lncRNAs interact with E3 ligase binding sites to substrates, thus affecting specific substrate protein degradation. To date, *SLC7A11-AS1* is, to the best to our knowledge, the first lncRNA reported that can disrupt $SCF^{\beta\text{-}TRCP}$ E3 complex formation, thus affecting the degradation of an extensive number of proteins that are important for cancer progression. Our work highlights the important role of *SLC7A11-AS1* in regulating β-TRCP1 function.

In summary, our work demonstrates that *SLC7A11-AS1* promotes cancer stemness and chemoresistance by blocking the nuclear NRF2 protein degradation through interaction with β-TRCP1. Our study suggests that *SLC7A11-AS1* may be of potential value as a novel therapeutic target for PDAC treatment.

MATERIALS AND METHODS

Cell Culture

Human PDAC cell lines BxPC-3, PANC-1, and AsPC-1 were cultured in RPMI-1640 medium (GIBCO, Gaithersburg, MD, USA) supplemented with 10% fetal bovine serum (GIBCO) and 1% penicillin/streptomycin. CFPAC-1 and 293T cells were cultured in Iscove's modified Dulbecco's medium (GIBCO) and Dulbecco's modified Eagle's medium (GIBCO), respectively, with the same supplement as shown above. The gemcitabine-resistant subline BxPC-3-

loading control and expressed relative to sh-Ctrl. (H) Western blot analysis of nuclear and cytoplasmic fractions from *SLC7A11-AS1*-knockdown and control PANC-1 cells treated with or without MG132 (1 μM) for 24 h. (I) Quantification of nuclear NRF2 as in (H) (n = 3). (J–L) PANC-1 cells with or without siRNA-mediated NRF2 knockdown were transfected with *SLC7A11-AS1* or empty vector for 48 h, followed by ROS detection using flow cytometry (J), qRT-PCR analysis of NRF2 target genes, *HMOX1* (K), and *GCLM* (L). *$p < 0.05$, **$p < 0.01$, ***$p < 0.001$. ns, not significant.

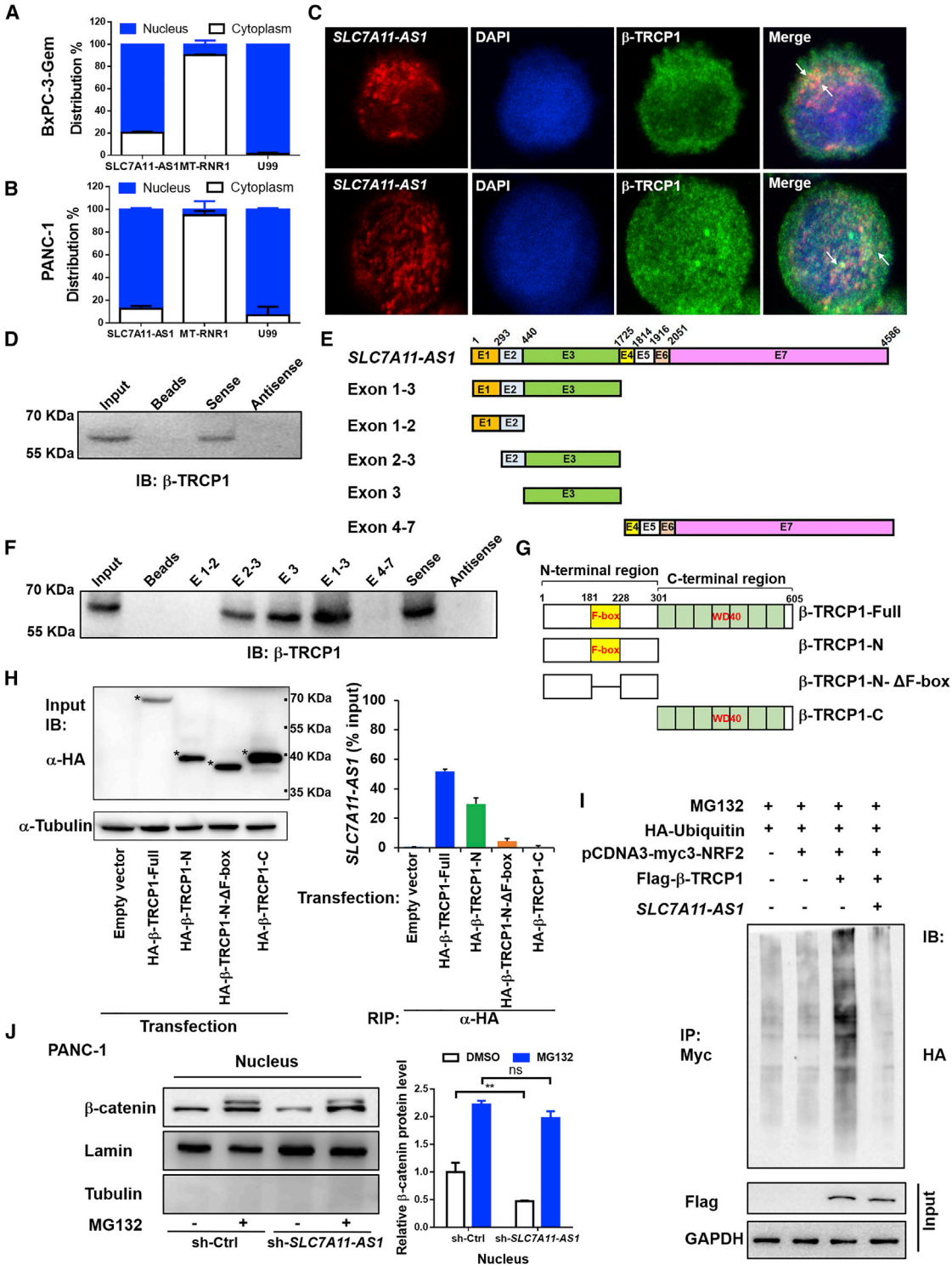

Figure 6. *SLC7A11-AS1* Prevents β-TRCP1-Mediated Ubiquitination and Degradation of NRF2

(A and B) Subcellular distribution of *SLC7A11-AS1* was detected by qRT-PCR in (A) BxPC-3-Gem and (B) PANC-1 cells. U99 and MT-RNR1 were as nuclear and cytoplasmic marker, respectively (n = 3). (C) The immunofluorescence staining of *SLC7A11-AS1* (red), β-TRCP1 (green), and DAPI (blue) in BxPC-3-Gem and PANC-1 cells. (D) Nuclear extracts from BxPC-3-Gem cells were incubated with biotinylated sense and antisense *SLC7A11-AS1* generated *in vitro*, and proteins were precipitated with streptavidin

(legend continued on next page)

Gem was maintained in medium containing 50 nM gemcitabine (LC Laboratories, Woburn, MA, USA).[20]

PDAC Patient Samples

PDAC samples and adjacent non-tumor tissues were obtained from patients diagnosed with PDAC at the Affiliated Tumor Hospital of Harbin Medical University (Harbin, China). All samples were collected immediately from resection, snap frozen in liquid nitrogen, and stored at −80°C. Written consent was obtained from all patients. Ethical consent was approved by the Committees for Ethical Review of Research involving Human Subjects of Harbin Medical University.

RNA Isolation and qRT-PCR

Total RNA was isolated using TRIzol (Invitrogen, Grand Island, NY, USA) and reverse transcribed into cDNA using a reverse transcription kit (TOYOBO, Japan). qRT-PCR was performed using GoTaq qPCR Master Mix (Promega, Madison, WI, USA) with gene-specific primers (Comate Bioscience, China) listed in Table S1. The results were calculated using the $2^{-\Delta\Delta Ct}$ method and normalized against internal control.

Transfection of Plasmid and Small siRNA

Transfection experiments were conducted by using Lipofectamine 3000 (Invitrogen) and blended within Opti-MEM I Reduced Serum Media (GIBCO). siRNA targeting *SLC7A11-AS1* (RiboBio, China) or *NRF2* (GenePharma, China) was transfected at the final concentration of 50 nmol/L. PCDNA3-myc3-NRF2 and HA-ubiquitin were provided by Profs. Ying Hu and Yu Li, respectively (Harbin Institute of Technology). Primers for plasmid construction and siRNA sequences were listed in Table S1.

Lentivirus Production and Infection

To establish stable knockdown cell lines, we cloned a short hairpin RNA (shRNA) sequence that specifically targets *SLC7A11-AS1* into pLKO.1-Puro vector (Addgene, Cambridge, MA, USA). The sequence of shRNA was listed in Table S1. Lentivirus was produced in 293T cells co-transfected with pCMV-VSV-G (vesicular stomatitis virus G protein) (1 μg), pGag/Pol/PRE (9 μg), and pLKO.1-puro empty or pLKO.1-puro-sh-*SLC7A11-AS1* plasmid (10 μg). The medium containing lentivirus was collected every 24 h and filtered (0.45 μm). Gemcitabine-resistant BxPC-3-Gem, PANC-1, and AsPC-1 cells were incubated with the medium for 48 h, and stable lines were selected using 10 μg/mL of puromycin (Sigma). The knockdown efficiency was evaluated by qRT-PCR.

Sphere-Formation Assay

Cells (500 cells/well) were seeded into six-well low-attachment plates (Corning, Tewksbury, MA, USA) and cultured in Dulbecco's modified Eagle's medium-F12 medium (GIBCO), containing 2% B27 (GIBCO), 10 ng/mL of epidermal growth factor (EGF; GIBCO), and 10 ng/mL of basic fibroblast growth factor (FGF; GIBCO) for 7 days. Spheroids were photographed.

MTT Assay

3-(4, 5-dimethylthiazolyl-2)-2, 5-diphenyltetrazolium bromide (MTT) was performed as described previously.[20] In brief, PDAC cells were seeded in 96-well plates (5×10^3 cells/well) and treated with various doses of gemcitabine for 72 h. MTT (5 mg/mL; Sigma) was added into each well after treatment, and the formed MTT products were dissolved in DMSO (Sigma). The optical density was measured at a wavelength of 490 nm using an iMark Microplate Absorbance Reader (Bio-Rad, USA). The half-maximal inhibitory concentration (IC_{50}) value was determined by using GraphPad 6 software (Prism). All of the experiments were performed in triplicate.

Colony Formation Assay

Cells seeded in six-well plates (500 cells/well) were treated with gemcitabine (1 μM) and continuously cultured for 14 days without disturbance. Culture medium was replaced every 5 days. Colonies were fixed in formaldehyde for 30 min, stained with 0.1% crystal violet for 30 min, and photographed.

ROS Detection

Cellular ROS level was measured by incubating cells with 2′, 7' dichlorodihydrofluorescein diacetate (DCFH-DA; 10 μM; Beyotime, China) for 30 min at 37°C after treatments. The reduced DCFH-DA can be oxidized and converted into fluorescent 2′, 7'-dichlorofluorescein (DCF) by intracellular ROS. Fluorescence intensity of cell suspension was determined by FCM (BD FACSCalibur; BD Biosciences). In total, 10,000 cells were analyzed per sample.

For ROS detection in tumor tissue, frozen tumors were sectioned into 10 μm, and the slides were incubated with dihydroethidium (DHE; 5 μM; Vigorous, China) in a humidified condition at 37°C for 30 min.[46] The fluorescent signals were detected by using a fluorescence microscope. The resulting DHE-mediated fluorescence was quantified by ImageJ.

beads and subjected to immunoblotting (IB) analysis with anti-TRCP1 antibody. (E) A schematic diagram of full-length *SLC7A11-AS1* and its series of truncates. (F) Nuclear extracts from BxPC-3-Gem cells were incubated with biotinylated *SLC7A11-AS1* truncates and antisense *SLC7A11-AS1* generated *in vitro*, and proteins were precipitated with streptavidin beads and subjected to IB analysis with anti-TRCP1 antibody. (G) A schematic diagram of β-TRCP1 and its truncates. (H) RIP assay analysis of the interaction of β-TRCP1 and its truncates (β-TRCP1-N, β-TRCP1-N-ΔF-box, and β-TRCP1-C) with *SLC7A11-AS1* in PANC-1 cells. Whole-cell expression (input) of proteins was detected by IB with indicated antibodies (left). The asterisks indicate β-TRCP1 and its truncates bands. The immunoprecipitated *SLC7A11-AS1* by using anti-HA antibody was measured by qRT-PCR and represented as a fraction of input RNA (% input) prior to immunoprecipitation (right) (n = 3). (I) Effect of *SLC7A11-AS1* on β-TRCP1-mediated ubiquitination of NRF2. 293T cells co-transfected with indicated plasmids were treated with MG132 (1 μM) for 12 h and subjected to immunoprecipitation (IP) with the anti-Myc antibody, followed by IB with anti-HA antibody. Whole-cell expression (input) of proteins was detected by IB with anti-FLAG or anti-GAPDH antibodies. (J) *SLC7A11-AS1* prevents β-catenin proteasomal degradation. Western blot (left) analysis of nuclear β-catenin in *SLC7A11-AS1*-knockdown and control PANC-1 cells treated with or without MG132 (5 μM) for 24 h. Quantification of β-catenin protein (right) was normalized to the loading control (Lamin) and expressed relative to sh-Ctrl without MG132 (n = 3). **p < 0.01. ns, not significant.

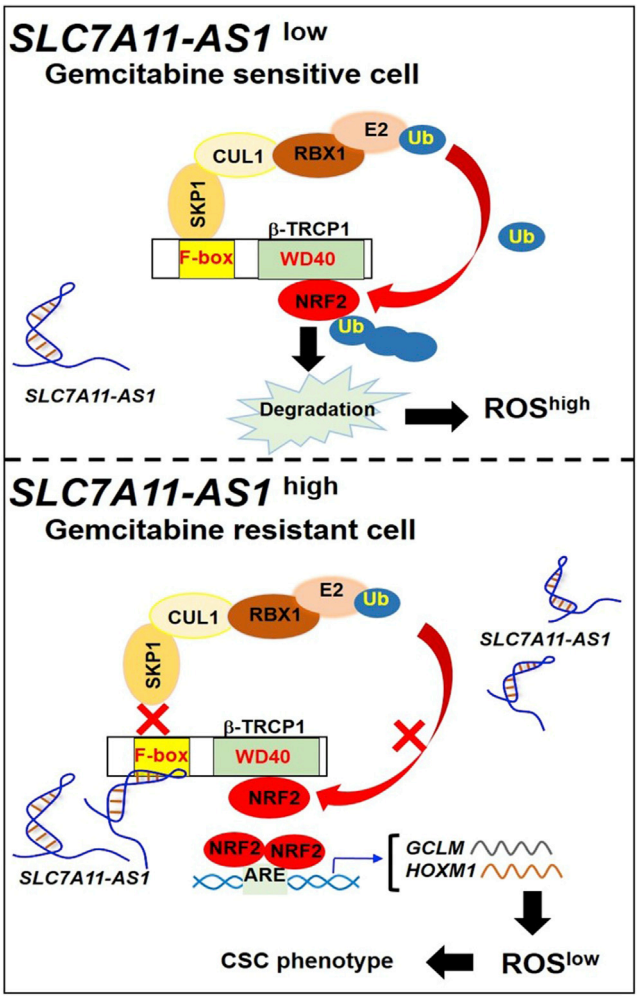

Figure 7. A Proposed Working Diagram of *SLC7A11-AS1*

SLC7A11-AS1 stabilizes NRF2 by interacting with β-TRCP1 to lower ROS for the maintenance of PDAC stemness.

Subcellular Fractionation

The nuclear and cytoplasmic fractions were prepared as described previously.[47] In brief, PANC-1 and BxPC-3-Gem cells were washed with cold PBS twice and resuspended in pre-chilled cell disruption buffer (1.5 mM $MgCl_2$, 10 nM KCl, 20 mM Tris-HCl, 1 mM DTT). Cell suspensions were incubated on ice for 10 min, followed by homogenization and addition of 0.1% Triton X-100. The homogenates were visually inspected under a microscope to ensure that the nuclei remained intact while the membranes were broken in over 90% of cells. The nuclei were separated from the cytosol by centrifuging at 1,500 × *g* for 5 min.

Western Blot Analysis

Whole-cell lysates were prepared using RIPA lysis buffer (50 mM Tris-HCl [pH 8.0], 150 mM sodium chloride, 1.0% Nonidet P-40 [NP-40], 0.1% SDS) with 1% protease inhibitor cocktail. Western blot was performed as described previously[20] with primary antibodies against NRF2, Nanog, Oct4, β-Catenin, GAPDH, α-Tubulin, FLAG tag (Proteintech, China), and Lamin (Santa Cruz, Dallas, TX, USA).

RNA Pull-Down Assay

For RNA *in vitro* transcription, full-length *SLC7A11-AS1* and its truncates were amplified and inserted into Peasy-T1 (TransGen, China). Linearized fragments were used as a template for *in vitro* transcription of biotin-labeled RNAs by using TranscriptAid T7 High Yield Transcription Kit (Thermos Scientific, Pittsburgh, PA, USA) and Label IT Nucleic Acid Labeling Kit (Mirus, Madison, WI, USA). After denaturing for 10 min at 65°C, the labeled transcripts (5 μg) were incubated with nuclear extracts (2 mg) with 100 U/mL RNaseOUT (Invitrogen) at 4°C with rotation. Unlabeled RNA with nuclear protein was used as control. After 2-h incubation, streptavidin beads (MedChemExpress [MCE]; Monmouth Junction, NJ, USA) were added, and the enriched components were analyzed by western blot.

RNA *In Situ* Hybridization and Immunofluorescence Staining

Biotin-labeled *SLC7A11-AS1* probe (1,420 nt in exon 3) was generated as described above. Cells were fixed with 4% paraformaldehyde for 15 min, followed by permeabilization with 0.1% Triton X-100 for 5 min and hybridization with biotin-labeled *SLC7A11-AS1* probe in 2× saline sodium citrate (SSC; Sigma) at 65°C overnight in a moist chamber.

For co-localization study, cells were co-stained with rabbit anti-β-TRCP1 antibody (1:100 dilution; ABclonal, China) and streptavidin, Alexa Flour 555 conjugate (1:200 dilution; Thermo Fisher) at 37°C for 1 h, then washed with PBS three times, and incubated with Chicken anti-Rabbit IgG (H+L) Cross-Adsorbed Secondary Antibody, Alexa Fluor 488 (1:200 dilution, Thermo Fisher) for 2 h at room temperature. The nuclei were counterstained with DAPI (Sigma). The fluorescence images were taken by confocal microscope.

RIP Assay

Full-length β-TRCP1 and its truncations (β-TRCP1-N, β-TRCP1-C) were amplified and sub-cloned into pIRM-3xHA vector using appropriate restriction enzyme digestion. β-TRCP1-N-ΔF-box was generated using two-stepwise PCR. HA-empty vector, HA-β-TRCP1, and its truncations were transfected into PANC-1 cells in the presence of *SLC7A11-AS1* expression vector PCDNA3.1-*SLC7A11-AS1* for 48 h. Cells were lysed with 1 mL buffer (150 mM NaCl, 1 mM EDTA, 20 mM HEPES, 1% NP-40, 1 mM PMSF, 1 mM DTT, 100 U/mL RNaseOUT). 100 μL of supernatant was saved as input for qRT-PCR analysis, and another 100 μL of supernatant as input for western blot analysis. Cell lysates were immunoprecipitated with anti-HA-tag antibody (ABclonal) overnight. The precipitated RNAs were eluted with TRIzol and analyzed by qRT-PCR using *SLC7A11-AS1*-specific primers (Table S1). The amount of immunoprecipitated RNAs is represented as the percentile of the amount of input RNA (% input).

Ubiquitination Assay

293T cells were transfected with HA-ubiquitin along with PCDNA3-myc3-NRF2 and pCXN2-FLAG-β-TRCP1 in the presence or absence of PCDNA3.1-*SLC7A11-AS1* for 24 h, followed by treatment with MG132 (1 μM, MCE) for an additional 12 h. Collected cells were lysed in 100 μL of dilution buffer containing 10 mM Tris-HCl (pH 8.0), 2 mM EDTA, 150 mM NaCl and 1% Triton X-100, and an equal amount of cell lysis buffer (2% SDS, 150 mM NaCl, 10 mM Tris-HCl [pH 8.0]). The diluted samples were centrifuged at 20,000 × *g* for 30 min, and the supernatant (1.5 mg) was used for immunoprecipitation with anti-Myc antibody (Cell Signaling Technology, Danvers, MA, USA), followed by immunoblotting with anti-HA antibody.

Protein Half-Life Assay

Cells were treated with CHX (100 μg/mL; Sigma) for up to 60 min and lysed with RIPA buffer. Whole-cell lysates (20 μg) were separated by SDS-PAGE, and protein levels were measured by immunoblot.

Mice Xenograft Study

All of the animal care and experimental procedures were approved by the Animal Care and Use Committee of Harbin Institute of Technology. Female athymic BALB/c nude mice (4–5 weeks old) were obtained from Beijing HFK Bioscience. For *in vivo* ROS detection, sh-*SLC7A11-AS1* or sh-Ctrl cells (1.5×10^6) were injected subcutaneously into the left or right posterior flank of nude mice, respectively (n = 5). For chemoresistance study, cells were injected into the right side of the mice (n = 4). Tumor volumes were calculated using the equation: $V = a \times b^2/2$, where a is the largest diameter, and b is the perpendicular diameter to a.

Statistical Analysis

Statistical analysis was carried out using GraphPad software, v.6. Student's t test (two-tailed) was used when comparing only two groups. Differences between more than two groups were analyzed by using two-way ANOVA. Data are presented as the mean ± standard deviation (SD) and repeated from at least three independent experiments. $p < 0.05$ was considered to be statistically significant.

SUPPLEMENTAL INFORMATION

Supplemental Information can be found online at https://doi.org/10.1016/j.omtn.2019.11.035.

AUTHOR CONTRIBUTIONS

H.Y. and Q.Y. conceived the idea and designed the experiments. H.Y., Q.Y., and K.L. wrote the manuscript. Q.Y. and K.L. performed the experiments and analyzed the data. C.Z. generated PCDNA3.1-*SLC7A11-AS1*. Some of the experiments were performed with help from X.H., Y.M., X.L., and J.L.

CONFLICTS OF INTEREST

The authors declare no competing interests.

ACKNOWLEDGMENTS

This work was supported by National Natural Science Foundation of China (grants 81872439 and 31700780) and China Postdoctoral Science Foundation Funded Project (grant 2018T110281). We thank Drs. Y. Li and H. Nie for providing clinical samples.

REFERENCES

1. Adamska, A., Domenichini, A., and Falasca, M. (2017). Pancreatic ductal adenocarcinoma: current and evolving therapies. Int. J. Mol. Sci. *18*, 1338–1380.
2. Siegel, R.L., Miller, K.D., and Jemal, A. (2019). Cancer statistics, 2019. CA Cancer J. Clin. *69*, 7–34.
3. Hung, S.W., Mody, H.R., and Govindarajan, R. (2012). Overcoming nucleoside analog chemoresistance of pancreatic cancer: a therapeutic challenge. Cancer Lett. *320*, 138–149.
4. Ju, H.Q., Gocho, T., Aguilar, M., Wu, M., Zhuang, Z.N., Fu, J., Yanaga, K., Huang, P., and Chiao, P.J. (2015). Mechanisms of overcoming intrinsic resistance to gemcitabine in pancreatic ductal adenocarcinoma through the redox modulation. Mol. Cancer Ther. *14*, 788–798.
5. Zhang, Z., Duan, Q., Zhao, H., Liu, T., Wu, H., Shen, Q., Wang, C., and Yin, T. (2016). Gemcitabine treatment promotes pancreatic cancer stemness through the Nox/ROS/NF-κB/STAT3 signaling cascade. Cancer Lett. *382*, 53–63.
6. Diehn, M., Cho, R.W., Lobo, N.A., Kalisky, T., Dorie, M.J., Kulp, A.N., Qian, D., Lam, J.S., Ailles, L.E., Wong, M., et al. (2009). Association of reactive oxygen species levels and radioresistance in cancer stem cells. Nature *458*, 780–783.
7. Shi, X., Zhang, Y., Zheng, J., and Pan, J. (2012). Reactive oxygen species in cancer stem cells. Antioxid. Redox Signal. *16*, 1215–1228.
8. Ryoo, I.G., Lee, S.H., and Kwak, M.K. (2016). Redox modulating NRF2: a potential mediator of cancer stem cell resistance. Oxid. Med. Cell. Longev. *2016*, 2428153–2428166.
9. Hong, Y.B., Kang, H.J., Kwon, S.Y., Kim, H.J., Kwon, K.Y., Cho, C.H., Lee, J.M., Kallakury, B.V., and Bae, I. (2010). Nuclear factor (erythroid-derived 2)-like 2 regulates drug resistance in pancreatic cancer cells. Pancreas *39*, 463–472.
10. Lister, A., Nedjadi, T., Kitteringham, N.R., Campbell, F., Costello, E., Lloyd, B., Copple, I.M., Williams, S., Owen, A., Neoptolemos, J.P., et al. (2011). Nrf2 is overexpressed in pancreatic cancer: implications for cell proliferation and therapy. Mol. Cancer *10*, 37–49.
11. Harder, B., Jiang, T., Wu, T., Tao, S., Rojo de la Vega, M., Tian, W., Chapman, E., and Zhang, D.D. (2015). Molecular mechanisms of Nrf2 regulation and how these influence chemical modulation for disease intervention. Biochem. Soc. Trans. *43*, 680–686.
12. Furukawa, M., and Xiong, Y. (2005). BTB protein Keap1 targets antioxidant transcription factor Nrf2 for ubiquitination by the Cullin 3-Roc1 ligase. Mol. Cell. Biol. *25*, 162–171.
13. Chowdhry, S., Zhang, Y., McMahon, M., Sutherland, C., Cuadrado, A., and Hayes, J.D. (2013). Nrf2 is controlled by two distinct β-TrCP recognition motifs in its Neh6 domain, one of which can be modulated by GSK-3 activity. Oncogene *32*, 3765–3781.
14. DeNicola, G.M., Karreth, F.A., Humpton, T.J., Gopinathan, A., Wei, C., Frese, K., Mangal, D., Yu, K.H., Yeo, C.J., Calhoun, E.S., et al. (2011). Oncogene-induced Nrf2 transcription promotes ROS detoxification and tumorigenesis. Nature *475*, 106–109.
15. Müerköster, S., Arlt, A., Sipos, B., Witt, M., Grossmann, M., Klöppel, G., Kalthoff, H., Fölsch, U.R., and Schäfer, H. (2005). Increased expression of the E3-ubiquitin ligase receptor subunit betaTRCP1 relates to constitutive nuclear factor-kappaB activation and chemoresistance in pancreatic carcinoma cells. Cancer Res. *65*, 1316–1324.
16. Li, Z., Zhao, X., Zhou, Y., Liu, Y., Zhou, Q., Ye, H., Wang, Y., Zeng, J., Song, Y., Gao, W., et al. (2015). The long non-coding RNA HOTTIP promotes progression and gemcitabine resistance by regulating HOXA13 in pancreatic cancer. J. Transl. Med. *13*, 84–99.
17. Zhan, H.X., Wang, Y., Li, C., Xu, J.W., Zhou, B., Zhu, J.K., Han, H.F., Wang, L., Wang, Y.S., and Hu, S.Y. (2016). LincRNA-ROR promotes invasion, metastasis and tumor

growth in pancreatic cancer through activating ZEB1 pathway. Cancer Lett. *374*, 261–271.

18. Mello, S.S., Sinow, C., Raj, N., Mazur, P.K., Bieging-Rolett, K., Broz, D.K., Imam, J.F.C., Vogel, H., Wood, L.D., Sage, J., et al. (2017). *Neat1* is a p53-inducible lincRNA essential for transformation suppression. Genes Dev. *31*, 1095–1108.
19. Jiao, F., Hu, H., Han, T., Yuan, C., Wang, L., Jin, Z., Guo, Z., and Wang, L. (2015). Long noncoding RNA MALAT-1 enhances stem cell-like phenotypes in pancreatic cancer cells. Int. J. Mol. Sci. *16*, 6677–6693.
20. Gao, Y., Zhang, Z., Li, K., Gong, L., Yang, Q., Huang, X., Hong, C., Ding, M., and Yang, H. (2017). Linc-DYNC2H1-4 promotes EMT and CSC phenotypes by acting as a sponge of miR-145 in pancreatic cancer cells. Cell Death Dis. *8*, e2924.
21. Pastrana, E., Silva-Vargas, V., and Doetsch, F. (2011). Eyes wide open: a critical review of sphere-formation as an assay for stem cells. Cell Stem Cell *8*, 486–498.
22. Ma, S., Lee, T.K., Zheng, B.J., Chan, K.W., and Guan, X.Y. (2008). CD133+ HCC cancer stem cells confer chemoresistance by preferential expression of the Akt/PKB survival pathway. Oncogene *27*, 1749–1758.
23. Tang, Z., Li, C., Kang, B., Gao, G., Li, C., and Zhang, Z. (2017). GEPIA: a web server for cancer and normal gene expression profiling and interactive analyses. Nucleic Acids Res. *45* (W1), W98–W102.
24. Menegon, S., Columbano, A., and Giordano, S. (2016). The dual roles of NRF2 in cancer. Trends Mol. Med. *22*, 578–593.
25. Rojo de la Vega, M., Chapman, E., and Zhang, D.D. (2018). NRF2 and the Hallmarks of Cancer. Cancer Cell *34*, 21–43.
26. Kim, H.R., Kim, S., Kim, E.J., Park, J.H., Yang, S.H., Jeong, E.T., Park, C., Youn, M.J., So, H.S., and Park, R. (2008). Suppression of Nrf2-driven heme oxygenase-1 enhances the chemosensitivity of lung cancer A549 cells toward cisplatin. Lung Cancer *60*, 47–56.
27. Chen, L.L. (2016). Linking long noncoding RNA localization and function. Trends Biochem. Sci. *41*, 761–772.
28. Sun, Q., Hao, Q., and Prasanth, K.V. (2018). Nuclear long noncoding RNAs: key regulators of gene expression. Trends Genet. *34*, 142–157.
29. Wang, Z., Liu, P., Inuzuka, H., and Wei, W. (2014). Roles of F-box proteins in cancer. Nat. Rev. Cancer *14*, 233–247.
30. Ougolkov, A., Zhang, B., Yamashita, K., Bilim, V., Mai, M., Fuchs, S.Y., and Minamoto, T. (2004). Associations among β-TrCP, an E3 ubiquitin ligase receptor, β-catenin, and NF-kappaB in colorectal cancer. J. Natl. Cancer Inst. *96*, 1161–1170.
31. Cai, Q., Wang, S., Jin, L., Weng, M., Zhou, D., Wang, J., Tang, Z., and Quan, Z. (2019). Long non-coding RNA GBCDRlnc1 induces chemoresistance of gallbladder cancer cells by activating autophagy. Mol. Cancer *18*, 82–97.
32. Tu, Z., Schmöllerl, J., Cuiffo, B.G., and Karnoub, A.E. (2019). Microenvironmental regulation of long noncoding RNA LINC01133 promotes cancer stem cell-like phenotypic traits in triple-negative breast cancers. Stem Cells *37*, 1281–1292.
33. Yuan, J., Liu, Z., and Song, R. (2017). Antisense lncRNA As-SLC7A11 suppresses epithelial ovarian cancer progression mainly by targeting SLC7A11. Pharmazie *72*, 402–407.
34. Luo, Y., Wang, C., Yong, P., Ye, P., Liu, Z., Fu, Z., Lu, F., Xiang, W., Tan, W., and Xiao, J. (2017). Decreased expression of the long non-coding RNA SLC7A11-AS1 predicts poor prognosis and promotes tumor growth in gastric cancer. Oncotarget *8*, 112530–112549.
35. Peitzsch, C., Tyutyunnykova, A., Pantel, K., and Dubrovska, A. (2017). Cancer stem cells: The root of tumor recurrence and metastases. Semin. Cancer Biol. *44*, 10–24.
36. Niess, H., Camaj, P., Renner, A., Ischenko, I., Zhao, Y., Krebs, S., Mysliwietz, J., Jäckel, C., Nelson, P.J., Blum, H., et al. (2015). Side population cells of pancreatic cancer show characteristics of cancer stem cells responsible for resistance and metastasis. Target. Oncol. *10*, 215–227.
37. Wu, S., Lu, H., and Bai, Y. (2019). Nrf2 in cancers: A double-edged sword. Cancer Med. *8*, 2252–2267.
38. Hanada, N., Takahata, T., Zhou, Q., Ye, X., Sun, R., Itoh, J., Ishiguro, A., Kijima, H., Mimura, J., Itoh, K., et al. (2012). Methylation of the KEAP1 gene promoter region in human colorectal cancer. BMC Cancer *12*, 66–76.
39. Yoo, N.J., Kim, H.R., Kim, Y.R., An, C.H., and Lee, S.H. (2012). Somatic mutations of the KEAP1 gene in common solid cancers. Histopathology *60*, 943–952.
40. Ooi, A., Dykema, K., Ansari, A., Petillo, D., Snider, J., Kahnoski, R., Anema, J., Craig, D., Carpten, J., Teh, B.T., and Furge, K.A. (2013). CUL3 and NRF2 mutations confer an NRF2 activation phenotype in a sporadic form of papillary renal cell carcinoma. Cancer Res. *73*, 2044–2051.
41. Rada, P., Rojo, A.I., Chowdhry, S., McMahon, M., Hayes, J.D., and Cuadrado, A. (2011). SCF/β-TrCP promotes glycogen synthase kinase 3-dependent degradation of the Nrf2 transcription factor in a Keap1-independent manner. Mol. Cell. Biol. *31*, 1121–1133.
42. Malloy, M.T., McIntosh, D.J., Walters, T.S., Flores, A., Goodwin, J.S., and Arinze, I.J. (2013). Trafficking of the transcription factor Nrf2 to promyelocytic leukemia-nuclear bodies: implications for degradation of NRF2 in the nucleus. J. Biol. Chem. *288*, 14569–14583.
43. Xu, J., Zhou, W., Yang, F., Chen, G., Li, H., Zhao, Y., Liu, P., Li, H., Tan, M., Xiong, X., and Sun, Y. (2017). The β-TrCP-FBXW2-SKP2 axis regulates lung cancer cell growth with FBXW2 acting as a tumour suppressor. Nat. Commun. *8*, 14002–14017.
44. Lan, Y., Xiao, X., He, Z., Luo, Y., Wu, C., Li, L., and Song, X. (2018). Long noncoding RNA OCC-1 suppresses cell growth through destabilizing HuR protein in colorectal cancer. Nucleic Acids Res. *46*, 5809–5821.
45. Taniue, K., Kurimoto, A., Sugimasa, H., Nasu, E., Takeda, Y., Iwasaki, K., Nagashima, T., Okada-Hatakeyama, M., Oyama, M., Kozuka-Hata, H., et al. (2016). Long noncoding RNA UPAT promotes colon tumorigenesis by inhibiting degradation of UHRF1. Proc. Natl. Acad. Sci. USA *113*, 1273–1278.
46. Schluterman, M.K., Chapman, S.L., Korpanty, G., Ozumi, K., Fukai, T., Yanagisawa, H., and Brekken, R.A. (2010). Loss of fibulin-5 binding to β1 integrins inhibits tumor growth by increasing the level of ROS. Dis. Model. Mech. *3*, 333–342.
47. Rio, D.C., Ares, M., Jr., Hannon, G.J., and Nilsen, T.W. (2010). Preparation of Cytoplasmic and Nuclear RNA from Tissue Culture Cells. Cold Spring Harb. Protoc. 2010, pdb.prot5441.